

AD \_\_\_\_\_

GRANT NUMBER DAMD17-96-1-6151

TITLE: Biophysical Studies of the Type 1 Repeats of Human  
Thrombospondin-1 to Characterize the Structural Basis of its  
Angiostatic Effect

PRINCIPAL INVESTIGATOR: Kristin G. Huwiler  
Deane F. Mosher, M.D.

CONTRACTING ORGANIZATION: University of Wisconsin  
Madison, WI 53706

REPORT DATE: August 1998

TYPE OF REPORT: Annual

PREPARED FOR: Commander  
U.S. Army Medical Research and Materiel Command  
Fort Detrick, Frederick, Maryland 21702-5012

DISTRIBUTION STATEMENT: Approved for public release;  
distribution unlimited

The views, opinions and/or findings contained in this report are those of the author(s) and should not be construed as an official Department of the Army position, policy or decision unless so designated by other documentation.

DTIC QUALITY INSPECTED 4

# REPORT DOCUMENTATION PAGE

*Form Approved*  
**OMB No. 0704-0188**

Public reporting burden for this collection of information is estimated to average 1 hour per response, including the time for reviewing instructions, searching existing data sources, gathering and maintaining the data needed, and completing and reviewing the collection of information. Send comments regarding this burden estimate or any other aspect of this collection of information, including suggestions for reducing this burden, to Washington Headquarters Services, Directorate for Information Operations and Reports, 1215 Jefferson Davis Highway, Suite 1204, Arlington, VA 22202-4302, and to the Office of Management and Budget, Paperwork Reduction Project (0704-0188), Washington, DC 20503.

<b>1. AGENCY USE ONLY (Leave blank)</b>		<b>2. REPORT DATE</b> August 1998	<b>3. REPORT TYPE AND DATES COVERED</b> Annual (1 Aug 97 - 31 Jul 98)	
<b>4. TITLE AND SUBTITLE</b> Biophysical Studies of the Type 1 Repeats of Human Thrombospondin-1 to Characterize the Structural Basis of its Angiostatic Effect			<b>5. FUNDING NUMBERS</b> DAMD17-96-1-6151	
<b>6. AUTHOR(S)</b> Kristin G. Huwiler Deane F. Mosher, M.D.				
<b>7. PERFORMING ORGANIZATION NAME(S) AND ADDRESS(ES)</b> University of Wisconsin Madison, WI 53706			<b>8. PERFORMING ORGANIZATION REPORT NUMBER</b>	
<b>9. SPONSORING/MONITORING AGENCY NAME(S) AND ADDRESS(ES)</b> Commander U.S. Army Medical Research and Materiel Command Fort Detrick, Frederick, Maryland 21702-5012			<b>10. SPONSORING/MONITORING AGENCY REPORT NUMBER</b>	
<b>11. SUPPLEMENTARY NOTES</b>			19981210 130	
<b>12a. DISTRIBUTION / AVAILABILITY STATEMENT</b> Approved for public release; distribution unlimited			<b>12b. DISTRIBUTION CODE</b>	
<b>13. ABSTRACT (Maximum 200)</b> Thrombospondin-1 (TSP1) is a disulfide bonded trimer of 450 kD; each monomer contains three type 1 repeats (T1Rs). TSP1 has several documented functions including its role as an angiogenic inhibitor. TSP1 and TSP1 fragments that include the T1Rs cause an endothelial cell-specific inhibition of growth and migration. The T1Rs were expressed using the baculovirus protein expression system. Recombinant baculoviruses were generated that express the three T1Rs in tandem (P123) and the third T1R (P3) as secreted histidine-tagged fusion proteins. N-terminal sequencing of P123 and P3 confirmed that the signal sequence was homogeneously removed. Protein purity, molecular mass determination, and disulfide-bond content was determined using mass spectroscopy. Circular Dichroism (CD) was used to access secondary and tertiary structure. The far-UV CD spectra for P3 and P123 are marked by distinctive positive ellipticity that is lost by thermal denaturation. The near-UV CD spectra are positive and upon heating approach zero ellipticity. Fluorescence spectroscopy revealed that the tryptophans were quenched and the maximum emission wavelength was red-shifted upon treatment with either DTT or guanidine hydrochloride. These results indicate that the T1R encodes an independently folding protein module with spectral properties dominated by the conserved tryptophans.				
<b>14. SUBJECT TERMS</b> Breast Cancer  Thrombospondin-1, Angiogenesis, Protein Structure, Properdin, Fluorescence Spectroscopy, WSXWS motif			<b>15. NUMBER OF PAGES</b> 32	
			<b>16. PRICE CODE</b>	
<b>17. SECURITY CLASSIFICATION OF REPORT</b> Unclassified	<b>18. SECURITY CLASSIFICATION OF THIS PAGE</b> Unclassified	<b>19. SECURITY CLASSIFICATION OF ABSTRACT</b> Unclassified	<b>20. LIMITATION OF ABSTRACT</b> Unlimited	



#### IV. Table of Contents

I.	Front Cover	1
II.	Standard Form 298	2
III.	Foreword	3
IV.	Table of Contents	4
V.	Introduction	5
VI.	Body	9
VII.	Conclusions	18
VIII.	References	21
IX.	Appendices- Figures	22

## V. Introduction

### A. Subject and Purpose

Thrombospondin-1 (TSP1) is a member of a family of modular glyco-proteins including thrombospondin-2 (1), thrombospondin-3 (2), thrombospondin-4 (3), cartilage oligomeric matrix protein (4), and F-spondin (5). TSP1 is a disulfide-bonded trimer with an approximate molecular mass of 450KDa. The modular structure of trimeric TSP1 is illustrated in figure 1 and is based in part on the electron microscopy of rotary shadowed TSP1. The amino-terminus consists of a globular heparin-binding domain (6) and is followed by the central stalk region. The 70KDa central stalk region contains three types of domains which are also found in other proteins, these include a procollagen module, three properdin or type 1 repeats, and three EGF-like or type 2 repeats (6,7). The C-terminus of TSP1 is dependent on  $Ca^{++}$  for its structural integrity (7,8) and it contains the cell adhesion motif RGD.

TSP1 is synthesized and secreted by various cell types where it can become incorporated into the extracellular matrix (ECM). The ECM is an important modulator of cell proliferation, migration, and differentiation (9-12). Several investigations indicate that TSP1 is a normal component of the extracellular matrix of mammary tissue. The level and pattern of expression of TSP1 is altered by the developmental (13), lactational (13), and neoplastic (14) state of the mammary tissue. TSP1 is found deposited in the basement membrane of normal breast tissue (14) and is also found in breast milk (15). The expression of TSP1 is altered in neoplastic breast tissue. In contrast to normal breast tissue, increased levels of TSP1 was present in the basement membrane surrounding preinvasive tumors while TSP1 was absent along the progressing front of invasive ductal carcinomas (14). *In vitro* experiments have demonstrated that an increase in TSP1 mRNA and protein expression correlated with a decrease in malignant progression (16) and inhibition of metastases (17).

Metastasis of tumor cells is a multi-step process that includes angiogenesis. A reasonable hypothesis suggested to explain the inhibition of metastases and malignant progression is that the presence of TSP1 in the tumor micro-environment modulates an angiostatic effect (18-21). This idea is supported by a growing body of work that has shown TSP1, TSP1 fragments, and certain TSP1 conserved peptide sequences to exert an endothelial-specific inhibition of growth and migration.

Our lab is interested in further examining the cell-specific effect of TSP1 by localizing active regions of the molecule and cell surface receptors that interact with TSP1. Using the baculovirus system we have recombinantly expressed intact as well as portions of TSP1 such as the type 1 repeats. Our lab has shown that recombinantly expressed human TSP1 (hTSP1) type 1 repeats does inhibit migration of bFGF stimulated bovine adrenal microvascular endothelial

cells. This study seeks to define the structural basis for the angiostatic effect of the hTSP1 type 1 repeats.

Each hTSP1 monomer contains three type 1 repeats that are encoded for by individual exons (22) and which contain approximately sixty amino acids. An alignment of the three type 1 repeats in TSP1 is shown in figure 2. I will employ several biophysical methods in a comparative study of hTSP1 type 1 repeats in tandem (P123) and the third type 1 repeat (P3). I will utilize circular dichroism, fluorescence spectroscopy, mass spectroscopy, and X-ray crystallography. Large quantities, tens of milligrams, of highly purified protein is necessary for these experiments. I have expressed the three type 1 repeats of human TSP1 in tandem (P123) and the third type 1 repeat alone (P3) using the baculovirus system to meet these ends. Determination of the structure critical for activity could be used as a starting point for the design of small molecules which elicit the same function.

## **B. Previous Work**

The first year of my pre-doctoral training grant was August 1996-August 1997. The work I accomplished during this time was fully described in my first progress report, submitted August 1997. I have summarized these results below.

### Construction of pCOCO Baculovirus Transfer Vector

The pAcGP67A baculovirus transfer vector (PharMingen) was chosen as the starting point for construction of a baculovirus transfer vector. It contains the GP67 signal sequence 5' to the multiple cloning site (MCS). This signal sequence is under the control of the very strong polyhedrin promoter. The pAcGP67A vector was modified 3' to the MCS by the addition of a DNA sequence that encodes a thrombin cleavage site followed by a His-tag. The exact sequence for the cleavage site is shown in Figure 3. The digested product was purified and ligated into the pAcGP67A MCS at the XbaI and PpumI sites. The resulting transfer vector is termed pAcGP67.COCO or pCOCO. A graphical map of the pCOCO vector is shown in Figure 3.

### Cloning hTSP1 Type 1 Repeats into pCOCO Baculovirus Transfer Vector

The sequences encoding P123 and P3 were amplified from hTSP1 cDNA by the polymerase chain reaction (PCR). The forward primers introduced an XmaI site while the reverse primer added an XbaI site. Following restriction enzyme digestion and purification these PCR products were cloned into the XmaI and XbaI sites in the MCS of pAcGP67.COCO. The resulting baculovirus transfer vectors were used to generate recombinant baculoviruses that express the cDNA as a secreted fusion protein with a His-tag at the C-terminus.

### Generation of Recombinant Baculoviruses

Recombinant baculoviruses were generated using Baculogold (Pharmingen) linearized AcNPV viral DNA. Co-transfections into Sf9 cells with baculogold and P123.COCO or P3.COCO were performed using CellFectin (Gibco-BRL). Recombinant baculoviruses were cloned by plaque purification. High titer ( $1-5 \times 10^8$  pfu/ml) virus stocks were prepared using Sf9 cells.

### Purification of Type 1 Repeats

The fusion protein is directed to the secretory pathway by the amino terminal GP67 signal sequence. This allows the recombinant protein to be purified from the conditioned media. The carboxy-terminus of the fusion protein (COCO) contains a thrombin cleavage site and a series of six histidines. The His-tag allows the recombinant protein to be readily purified on nickel-chelate resin while the thrombin cleavage site allows the His-tag to be subsequently removed.

An outline of the **purification scheme** follows:

- Infect High 5 Cells @  $1 \times 10^6$  cells/ml with Recombinant Baculovirus.
- Incubate at 27°C for ~62 hours.
- Clarify Conditioned Media (CM) by centrifugation to remove Cell Debris.
- Incubate clarified CM in batch with NiNTA resin.
- Wash NiNTA resin with buffer containing 10mM Imidazole.
- Elute NiNTA Resin with buffer containing 250mM Imidazole.
- Pool Fractions containing Recombinant Protein.
- Dialyze Recombinant protein into Thrombin Reaction Buffer.
- Digest 1 milligram of Recombinant Protein with 2-4 units of Biotinylated Thrombin.
- Incubate digest at room temperature for ~18 hours.
- Remove Biotinylated Thrombin by incubating Digest with Streptavidin Resin.
- Incubate with NiNTA Resin to remove uncleaved recombinant protein.
- Dialyze into Tris-buffered saline, pH 7.5.
- Concentrate by Ultra-filtration.

A graphical representation of the fusions expressed and the expected sizes are shown in figure 4. Yields in excess of 20ug of fusion per milliliter of conditioned media were obtained for P123.COCO. The level of expression (1-5ug/ml) of P3.COCO was substantially lower than that obtained for P123.COCO even after examining more than 10 clones of P3.COCO and optimizing infection conditions.

### N-terminal Sequencing of P123.COCO

The COCO fusion proteins are expressed with the 38 amino acid long GP67 signal sequence. In order to determine if the fusion proteins had the GP67 signal sequence removed at the predicted cleavage site and to determine whether the signal sequence site was homogeneous, N-terminal sequencing of P123.COCO was initiated. The P123.COCO sample was determined to have a homogeneous N-terminus beginning at the anticipated amino acid, based on the predicted signal sequence cleavage site.

### Glycosylation of P123

The third type 1 repeat of human TSP1 contains a site (N-X-S/T) for N-linked glycosylation. The DIG Glycan Detection (Boehringer Mannheim) system has been used to determine if baculovirally expressed P123 is glycosylated. Manufacturer's instructions for detecting glycosylation of immobilized proteins were followed. Both P123 expressed as COCO or GELEX fusions were tested. The result of this analysis shows that P123 expressed in either the COCO or GELEX expression systems is glycosylated.

### Initial Characterization of P3 by Circular Dichroism

The University of Wisconsin-Madison Biophysics Instrumentation Facility's AVIV 62 ADS circular dichroism spectrophotometer was used to monitor the far-UV CD signal for P3. The P3 sample was 0.19 mg/ml in 10mM Potassium Phosphate, 100mM Sodium Chloride, pH 7.3 and was placed in a quartz cuvette of pathlength 0.1cm. A CD spectra was obtained by scanning from 260nm to 195nm at 25°C. A temperature scan from 25°C to 70°C was also performed on the P3 sample. The CD signal at 229nm and the total fluorescence emission when exciting at 291nm was monitored. The temperature was increased in 5°C increments using a slope of 50°C/min and an equilibration time of one minute.

The far-UV CD spectra of P3 is marked by distinctive positive ellipticity above ~202nm. The protein properdin contains six TSP1 type 1 repeats which compose ~80% of the primary sequence. The far-UV CD spectrum of properdin (23) is positive above ~195nm and has a similar shape to that of P3. The secondary structure of recombinant TSP1 type 1 repeat appears to be similar to that of natural properdin.

From the temperature scan of P3, it was observed that the CD signal monitored at 229nm decreased with increasing temperature with the change beginning between 45-50°C. Conversely, the total fluorescence of the sample increased with increasing temperature. The first significant change occurred between 45-50°C. The thermal denaturation of P3 is accompanied by an increase in the fluorescence, suggesting that the conserved tryptophans of P3 are quenched in the native state.

## **VI. Body**

### **A. Reasons for Altering the Purification Protocol for P3.COCO**

In section A (Previous Work) of the Introduction, I described the "COCO" baculoviral expression system that is used to produce the type 1 repeats. In summary, recombinant baculoviruses generated with the pCOCO transfer vector express the gene of interest as a fusion protein with a series of six histidines at the C-terminus. In addition, the GP67 signal sequence is 5' and in frame with the gene of interest in the pCOCO transfer vector. The presence of the signal sequence directs the protein to the secretory pathway and allows the protein to be purified from the conditioned media. The presence of the His-tag at the C-terminus allows for affinity purification of the recombinant fusion protein on nickel resin (NiNTA). The expression and purification of the type 1 repeats using the COCO system was initially determined using the construct containing the three type 1 repeats in tandem (P123.COCO).

As described in Section A of the Introduction, P123.COCO is expressed at 20-50ug/ml while P3.COCO was expressed at 1-5ug/ml. The lower level of expression of P3.COCO presented problems when scale-up was undertaken in order to purify milligram quantities of the P3.COCO. I have found that when the His-tagged protein is expressed at low concentrations, the protein fails to bind the nickel resin efficiently. In order to increase the strength of the interaction between the His-tag and the NiNTA, I initially tried raising the pH of the conditioned media to ~8.0. The pH of the conditioned baculovirus media is ~6.3. I dialyzed the clarified conditioned media into sodium phosphate buffer in the presence of sodium chloride at pH 8.0. This was not only tedious since I was working with at least 1 liter of conditioned media, but it also failed to improve the purification yields. The procedure that I determined to work consistently for P3.COCO, which is secreted at low levels, is the concentration of the conditioned media prior to incubation with the NiNTA. The protocol is described below.

### **B. Experimental Methods**

#### Purification of the Third Type 1 Repeat (P3.COCO)

High 5 cells (BTI-TN-5B1-4) were grown at 27°C in using SF900 II serum free media. For large scale production, four liter shaker flasks were used. Cells were infected at a density of  $1 \times 10^6$  cells/ml. A multiplicity of infection (MOI) of 2 was routinely used and the infection was allowed to proceed for ~62 hours.

Since P3.COCO is directed to the insect secretory pathway by the GP67 signal sequence, the first step in the purification procedure involves clarifying the conditioned media (CM). The insect cells are pelleted at ~8000xg for 10 minutes. The CM is carefully decanted from the cell pellet and imidazole, pH 6.7, is added to a final concentration of 10mM. PMSF is then added to a final concentration of 2mM.

The second step involves the concentration of the CM using ultrafiltration. Prior to concentration, the CM is filtered through Whatman No.2 filter paper which possesses a particle retention of 8 $\mu$ m. The filtered CM is then concentrated using an Amicon CH2S Spiral Wound Cartridge ultrafiltration system. An S3Y3 spiral wound cartridge is used and it has a surface area of 2.5 ft<sup>2</sup> and a molecular weight cut-off of 3,000 Da. For most of the run, the system is run with a pump speed of 7-8 and a back-pressure of ~20psi. The media is concentrated at least 10-20 fold. The concentrated media is then centrifuged at 15,000xg for 15 minutes.

The third step involves incubation of the clarified concentrated CM in batch with NiNTA resin (Qiagen). The concentrated CM is transferred to 50 ml conical tubes and equilibrated NiNTA resin is added. The amount of resin to use is determined by the expression levels of the fusion protein. The tubes are mixed on a nutator and the incubation proceeds for 1-2 hours.

The fourth step involves washing and eluting the protein from the NiNTA resin. Using a clinical centrifuge, the resin is pelleted in the 50ml conical tubes at <500rpm for ~3 minutes. The media was carefully removed from the settled resin using a pipet. The NiNTA was washed one time with 10mM Tris, pH 7.4, 500mM NaCl, 10mM Imidazole and then transferred to a column. The flow was adjusted to 0.5ml/min and allowed to rinse with this solution until baseline was reached. The column was then washed with a 10mM Tris, pH 7.4, 500mM NaCl, 15mM imidazole solution until a new baseline was reached. The column was eluted with 10mM Tris, 300mM NaCl, 250mM imidazole pH 7.4. The fusion protein is eluted within the first four column volumes with the majority of fusion in the second column volume.

The fifth step in the purification of the recombinant protein involves removal of the His-tag by proteolytic cleavage with thrombin. The fractions from the NiNTA column were pooled and dialyzed at 4°C against thrombin reaction buffer (50mM Tris-Cl, 150mM NaCl, 2.5mM CaCl<sub>2</sub>, pH 8.5). The conditions necessary to remove the His-tag using biotinylated-thrombin (Novagen) were determined. An 18-20 hour digestion at room temperature using 2-4 units thrombin/mg of fusion was sufficient. The biotinylated thrombin was removed using Streptavidin-agarose (Novagen) according to the manufacturer's instructions. In order to remove any incompletely digested fusion protein, the sample was incubated with NiNTA resin in batch; it was separated from the resin by pouring through a column. The resulting sample was adjusted to 0.02% sodium azide and 2mM Pefabloc SC. The recombinant protein was dialyzed into TBS at 4°C and subsequently concentrated using a Centriplus 3 (Millipore) ultrafiltration device.

#### N-terminal Sequencing of P3.COCO

Purified P3.COCO was denatured, reduced, and run on a 14% SDS-PAGE. The protein was transferred to PVDF and the blot was stained with 0.1% Amido Black. The N-terminal sequencing was performed in the lab of Dr. Johan Stenflo, Lund University, Sweden. The sample underwent >10 cycles of sequencing.

#### Molecular Mass determination of P3 and P123 by MALDI-TOF

Both P3 and P123 proteins were extensively dialyzed against 5% acetic acid at 4°C and then lyophilized. The proteins were resuspended in water to a concentration of 10-40pmol/ul. The matrix was  $\alpha$ -cyano-4-hydroxycinnamic acid at 10mg/ml. The data were collected on a Bruker matrix-assisted laser desorption time-of-flight (MALDI-TOF) mass spectrometer at the University of Wisconsin- Madison, Department of Chemistry. Internal calibrants of insulin, ubiquitin, and/or trypsinogen were used to determine the masses.

#### Glycosylation of P3.COCO

The DIG Glycan Detection (Boehringer Mannheim) system has been used to determine if baculovirally expressed P3 is glycosylated. Manufacturer's instructions for detecting glycosylation of immobilized proteins were followed.

#### Determination of the Disulfide Bond Content of P3 using MALDI-TOF

The P3 protein was labeled for 30 minutes with Iodoacetic Acid (IA) under four conditions: Native; 6mM DTT; 6M Guanidine Hydrochloride; and 6M Guanidine Hydrochloride plus 6mM DTT. The protein was equilibrated in each of the four conditions for 90 minutes under nitrogen gas prior to labeling with IA. Following labeling, the proteins were dialyzed extensively against 5% acetic acid at 4°C and then lyophilized. The proteins were resuspended in water to a concentration of 10-40pmol/ul. The matrix was  $\alpha$ -cyano-4-hydroxycinnamic acid at 10mg/ml. The data were collected on a Bruker MALDI-TOF mass spectrometer at the University of Wisconsin- Madison, Department of Chemistry. Internal calibrants of insulin and ubiquitin were used to determine the masses.

#### Far-UV Circular Dichroism of P3 and P123

The University of Wisconsin-Madison Biophysics Instrumentation Facility's AVIV 62 ADS circular dichroism spectrophotometer was used to monitor the far-UV CD signal for P3 and P123. The P3 and P123 samples were dialyzed against 10mM Potassium Phosphate, 100mM Sodium Chloride, pH 7.5. A quartz cuvette of pathlength 0.1cm was used for data collection. Spectra were collected at temperatures between 25°C-65°C. The CD spectra were obtained by scanning from 260nm to at least 200nm. A minimum of three scans per temperature were collected and averaged. All data were baseline corrected and converted to molar ellipticity, mean residue weight ( $\Theta$ MRW).

### Near-UV Circular Dichroism of P3 and P123

The University of Wisconsin-Madison Biophysics Instrumentation Facility's AVIV 62 ADS circular dichroism spectrophotometer was used to monitor the near-UV CD signal for P3 and P123. The P3 and P123 samples were dialyzed against 10mM Tris-Cl, 150mM Sodium Chloride, pH 7.5. A quartz cuvette of pathlength 1cm was used for data collection. Spectra were collected at temperatures between 25°C-65°C. The CD spectra were obtained by scanning from 340nm to 240nm. A minimum of three scans per temperature were collected and averaged. All data were baseline corrected and converted to molar ellipticity, mean residue weight ( $\Theta$ MRW).

### Dual Monitoring of CD and Fluorescence Signals of P123 with Increasing Temperature

The University of Wisconsin-Madison Biophysics Instrumentation Facility's AVIV 62 ADS circular dichroism spectrophotometer was used to monitor the far-UV CD signal at 210nm and the total fluorescence emission when an excitation wavelength of 284nm was used. The P123 samples was dialyzed against 10mM Potassium Phosphate, 100mM Sodium Chloride, pH 7.5. A quartz cuvette of pathlength 0.1cm was used for data collection. The temperature was scanned from 25°C to 75°C. The temperature was increased in 2°C increments using a slope of 50°C/min and an equilibration time of 1 minute. All data were baseline corrected.

### Fluorescence Emission Spectra of P3 and P123 under Native and Denaturing Conditions

The data were collected on an SLM 8000 spectrofluorometer using quartz cuvettes of 1cm pathlength. Four conditions for each protein were tested: Native, 10mM Tris-Cl, 150mM NaCl, pH7.5 (TBS); 10mM DTT in TBS; 6M Guanidine Hydrochloride in TBS; 6M Guanidine Hydrochloride and 10mM DTT in TBS. The temperature was held constant at 25°C. The protein concentration for P3 and P123 in each of the four conditions was held constant. The total absorbance at 280nm was below 0.1 O.D.. A minimum of three scans were collected and averaged per condition. In addition, the change in the maximum wavelength of emission was followed during a titration of P3 and P123 with DTT.

## **C. Results and Discussion**

### Purification of the third type 1 Repeat (P3.COCO)

Yields of 1-2mg of P3.COCO per liter of conditioned media were obtained. A time course of infection using three different MOIs revealed that an MOI=2 for ~62 hrs, yielded the best results. Longer incubations or excess virus resulted in cleavage of the His-tag from the protein during the infection. No loss of protein was found during the concentration of the CM using the

spiral wound membrane ultrafiltration system. P3.COCO was retained by the 3,000 MWCO filter during the concentration process, but it did not adhere to the filter.

The conditioned media from the baculovirus system contains proteins that will adhere non-specifically to the NiNTA because they possess surface histidines. The presence of imidazole during the incubation of CM with NiNTA will reduce the amount of non-His-tagged proteins that bind to the NiNTA. I found that more concentrated CM required higher concentrations of imidazole in order to reduce the non-specific binding. In general, the conditioned media was adjusted to 10-20mM Imidazole and 500mM NaCl. The conditions necessary to remove the His-tag using biotinylated-thrombin were determined. An 18-20 hour incubation at room temperature using 2-4 units thrombin/mg of P3.COCO resulted in >95% cleavage.

#### N-terminal Sequencing of P3.COCO

The COCO fusion proteins are expressed with the 38 amino acid long GP67 signal sequence. In order to determine if the fusion proteins had the GP67 signal sequence removed at the predicted cleavage site and to determine whether the signal sequence site was homogeneous, N-terminal sequencing of P3.COCO was initiated. Like P123.COCO, the P3.COCO sample was determined to have a homogeneous N-terminus beginning at the anticipated amino acid, based on the predicted signal sequence cleavage site. The results are presented in Figure 5.

#### Glycosylation of P3.COCO

The third type 1 repeat of human TSP1 contains a site (N-X-S/T) for N-linked glycosylation. The DIG Glycan Detection system has been used to determine if baculovirally expressed P123 is glycosylated. The three step method employs an enzyme immunoassay to detect sugars on immobilized protein. The result of this analysis shows that P3 expressed in the COCO expression system is glycosylated. In the previous report I showed that P123.COCO expressed in either the COCO or GELEX baculovirus expression systems is glycosylated as determined by this DIG Glycan assay.

#### Molecular Mass determination of P3 and P123 by MALDI-TOF

Representative MALDI-TOF Mass spectra of P3 and P123 are shown in Figure 7. The table in figure 7 summarizes the average mass of the peaks of P3 determined from greater than 10 independent measurements using insulin (5734.6Da) and ubiquitin (8565.9 Da) as internal calibrants. P3 appears as a minimum of 4 peaks which differ in mass by 156-164 Da. The mass difference between one peak and the next is on the order of the mass of a single sugar, ~162Da. Therefore, it is possible that these mass differences are due to the sequential addition of single sugars to the P3 protein. As discussed above, P3 appears to be glycosylated when analyzed

using the DIG Glycan Detection system. Although P3 contains a site for N-linked glycosylation (N-X-T), it is not expected to be utilized since the amino acid which occupies the X position in P3 is a proline. If the mass differences of 156-165Da is due to the sequential addition single sugars, then it is likely to be O-linked glycosylation rather than N-linked. Consistent with the idea that the difference in masses is due to the presence of O-linked glycosylation, I have seen no effect on P123 expressed by cells treated with tunicamycin, a specific inhibitor of N-linked glycosylation. I have attempted chemical removal of the carbohydrate with sodium borohydride, but the procedure resulted in complete fragmentation of the P3. I will try to confirm the presence of O-linked glycosylation using a chemical inhibitor of O-linked glycosylation that can be applied to the cells. The protein will then be analyzed by MALDI-TOF MS.

The expected mass of P3 based on the known N-terminus and the Thrombin cleavage site at the C-terminus is 7275 Da. This is ~20 Da smaller than that of the average mass of the first peak of P3.C. There are several modifications that could explain a loss of 17-18 Da. A few examples include conversion of a serine to a dehydroalanine (-18Da), or succinimide formation from aspartic acid (-18Da) or asparagine (-17Da). It is also possible that a point mutation occurred that could give rise to a loss of ~20 Da. However, I have no evidence to suggest this occurred and the cDNA was sequenced prior to cloning into the pCOCO transfer vector. I plan to sequence the recombinant baculovirus DNA that expresses P3 to confirm that no point mutations occurred.

The mass determination of P123 has been more difficult than that for P3. I have found it very difficult to get good signal and peaks that are well resolved. As seen in Figure 7, P123 appears as two poorly resolved peaks. It is likely that there are more peaks present that are currently unresolved. Due to the low signal and the relatively broad peaks, it has been difficult to get accurate masses. The average mass of the first peak of P123 is ~54 Da under the expected mass of P123 (19,973 Da). Interestingly, three modifications of -18Da, similar to that which I discussed above for P3, would account for the -54 Da seen for P123. This would imply that if there is a site (such as serine, aspartic acid, or asparagine) modified in the third type 1 repeat (P3), then there are analogous sites in the first and second type 1 repeats that are also modified. There are two places where serines are conserved in the three type 1 repeats: the serine in the second WSXW box of each type 1 repeat, and the residue following the first cysteine in each type 1 repeat is a serine. In addition there are two locations where aspartic acid (D) or asparagine (N) is found in each type 1 repeat: the third residue before the first tryptophan (W) is either a D or N, and the first residue after the third Cys is either a D or N in each of the type 1 repeats.

The difference in mass between the two peaks is 159Da. Again, this is similar to what is seen for P3 and is on the order of the addition of a single sugar. In the previous progress report, I provided data using the DIG Glycan detection method showing that P123 expressed in either the COCO or the GELEX expression system is positive for the presence of carbohydrate. In order to

improve the resolution of the P123 MS data, I am working on alternative methods to remove trace ions that might be sticking to the protein and interfering with MALDI-TOF MS. In addition, I have tried using matrices other than  $\alpha$ -cyano-4-hydroxycinnamic acid, but I have not consistently seen an improvement in the resolution of the data.

#### Determination of the Disulfide Bond Content of P3 using MALDI-TOF

Figure 8 summarizes the data obtained when the P3 protein was labeled with Iodoacetic acid (IA) under four conditions: Native, DTT treated, Guanidine Hydrochloride (GuHCl) treated, or DTT and Guanidine Hydrochloride (DTT/GuHCl) treated. This experiment is designed to determine if there are any free thiols present in P3 and the number of disulfide bonds. The table lists the mass of the first peak of P3 for each treatment condition. Only under reducing conditions, DTT or DTT/GuHCl, were cysteines labeled with IA. The number of cysteines labeled is determined by dividing the change in mass due to labeling by the mass of the label (IA). For both reducing conditions, 6 cys were labeled which is the number of Cys present in P3. Since denaturing P3 in 6M GuHCL and labeling with IA failed to cause a mass shift, there are no free thiols present. Therefore, all the cys in P3 are in disulfide bonds.

I have also tried this experiment with P123; however, I could not get good resolution of the data. As I mentioned above, I am working on improving the resolution with the native protein. Once this is determined, I will repeat this experiment on P123 to determine if all cys are in disulfide bonds.

#### Far-UV Circular Dichroism of P3 and P123

The far-UV CD spectra of a protein examines the secondary structure adopted by the protein backbone. Figures 9A and 9B shows the thermal denaturation of P3 and P123 monitored by CD in the far-UV. The proteins were equilibrated at each of the following temperatures: 25°C, 37°C, 45°C, 50°C, 55°C, 60°C, and 65°C. The spectra for P3 and P123 are marked by positive ellipticity that could be due in part to trp contribution. The two positive signals are also seen in the complement protein properdin which contains six type 1 repeats in series (23). Positive CD signal in the far-UV has been noted for other proteins with predominantly  $\beta$ -sheet and  $\beta$ -turn secondary structure that contain aromatic clusters (24,25).

The spectra at 25°C compared to that at 37°C for P3 or P123, are nearly identical. Therefore there is no change in secondary structure between 25°C and physiological temperature. Heating P3 or P123 causes a transition to a random coil conformation with the loss of secondary structure beginning at 45°C. As seen in Figure 9C, the far-UV CD spectra of P3 and P123 at 25°C plotted as molar ellipticity (mean residue weight) are very similar. The suggestion is that the overall secondary structure of the three modules in tandem is not significantly altered when compared to

the single module. However, P123 CD signal remains positive to ~199nm, while P3 crosses the zero at ~202nm.

#### Near-UV Circular Dichroism of P3 and P123

The near-UV CD spectra of a protein examines the chirality of the aromatic residues and disulfide bonds. Figure 10A and 10B shows the thermal denaturation of P3 and P123 monitored by CD in the near-UV. The proteins were equilibrated at each of the following temperatures: 25°C, 37°C, 45°C, 50°C, 55°C, and 65°C. The spectra for P3 and P123 are marked by positive ellipticity. The peak centered about 280nm is due to the trps, since neither P3 and P123 have tyrosine.

The spectra at 25°C compared to that at 37°C for P3 or P123, are nearly identical. Therefore there is no change in the chirality of the trp residues between 25°C and physiological temperature. Heating P3 or P123 to 55°C eliminates the chirality of the trps. As seen in Figure 10C, the near-UV CD spectra of P3 and P123 at 25°C plotted as molar ellipticity (mean residue weight) are very similar in shape. However, P123 is approximately two-thirds the intensity of P3. There is an overall difference in the chirality of the 9 trps in P123 compared to the three trps in P3.

#### Dual Monitoring of CD and Fluorescence Signals of P123 with Increasing Temperature

Figure 11 shows the dual monitoring of the P123 far-UV CD signal at 210nm and the total fluorescence emission when excitation occurs at 284 nm with increasing temperature. This allows the effect of thermal denaturation on the secondary structure and the effect on the trps to be simultaneously monitored. Heating P123 from 25°C->75°C causes a decrease in the CD signal at 210nm and an increase in the total fluorescence emission. The large decrease in fluorescence intensity seen above 60°C is simply a temperature effect on the fluorescence of trp. The unfolding of P123 appears to be cooperative. The mid-point of the transition due to increasing temperature is attained at a lower temperature for the fluorescence signal compared to the CD signal. These trends are similar to that which I reported in the last progress report for P3.

#### Fluorescence Emission Spectra of P3 and P123 under Native and Denaturing Conditions

Figure 12A and 12B shows the fluorescence emission spectra of P3 and P123 under four conditions: Native, 10mM Tris-Cl, 150mM NaCl, pH7.5 (TBS); 10mM DTT in TBS; 6M Guanidine Hydrochloride in TBS; 6M Guanidine Hydrochloride and 10mM DTT in TBS. Under native conditions, the wavelength of maximum emission ( $\lambda_{max}$ ) for P3 and P123 are very similar, 332-333nm (Figure 12C). The environment of the trps in P3 and P123 would be expected to be slightly non-polar based on this  $\lambda_{max}$ . Upon reduction of the disulfides with

DTT or denaturation of P3 or P123 with 6M GuHCl, there is a large enhancement in total fluorescence and a large red-shift in  $\lambda_{\max}$  (Figure 12C). The  $\lambda_{\max}$  emission under these conditions is ~350nm which is indicative of the trps being solvent exposed. In the native conformation, the disulfides appear to act as quenchers and the trps are in a less polar environment compared to the denatured or reduced state.

Figure 12D shows the change induced in  $\lambda_{\max}$  emission for P3 and P123 upon titration with DTT. The addition of 2-4 mM DTT resulted in the maximum change in  $\lambda_{\max}$  emission. This change was completed within 20 minutes at room temperature. By monitoring the fluorescence it is clear that disulfide bond reduction alters the environment of the trps. I have begun preliminary investigations into the effect of DTT on P3 secondary structure by monitoring the far-UV CD signal. Addition of 2mM DTT caused a slow loss of secondary structure. After 2.5 hours in 2mM DTT at 25°C, a wavelength scan in the far-UV revealed that P3 still retained some of its secondary structure. Heating the reduced P3 sample to 45°C resulted in complete elimination of secondary structure. At this point it appears that the disulfides strongly contribute to maintaining the environment of the trps and the effect of reduction is seen in minutes of the addition of DTT. Also, the disulfides appear to contribute to the thermal stability of the secondary and tertiary structure of P3. However, the effect of reduction on secondary structure is slow at 25°C and takes hours to reach completion.

#### **D. Recommendations in Relation to the Statement of Work**

The expression of the type 1 repeats as His-tag fusions using the COCO baculovirus system was described in my previous progress report as a solution to utilizing the GELEX baculovirus system. The COCO system has allowed me to meet many of the goals I had originally set. However, no system is perfect and one of the limits of the COCO system was encountered when expressing P3 in large scale. Very dilute solutions of His-tagged proteins (<5ug/ml) fail to bind the NiNTA resin from baculoviral conditioned media. It was necessary to spend a great deal of time to overcome this problem. The problem was not immediately apparent and many areas were investigated. I was able to set-up a system using a spiral-wound cartridge ultrafiltration device that could concentrate the clarified conditioned media at greater than 3 liter per hour and subsequently allow the purification of the P3 protein on the NiNTA resin. The affinity of the His-tagged proteins, and all proteins containing several surface histidines in the conditioned media, increased for NiNTA upon concentration of the conditioned media. In order to attain clean preparations of His-tagged protein, it was necessary to substantially increase the amount of imidazole used in the initial incubation of concentrated CM with NiNTA. In addition, the

stringency of the washing conditions of the NiNTA had to be increased when using concentrated CM.

The problems encountered with the GELEX protein expression system and some with expressing P3 in the COCO system has slightly set back my progress. However, I have completed the bulk of the work on the basic biophysical characterization of the type 1 repeats. I have completed technical objective one for P3 and P123 since I have a system in place that has proven to allow the large scale production of both of these proteins. I have completed technical objective two, the use of CD to analyze the secondary structure, for both P3 and P123.

I have begun technical objectives 3 and 4 for P3 and P123 which involve conformational studies using fluorescence spectroscopy and CD. I have examined the effect of temperature on the far-UV CD, near-UV CD, and fluorescence signals. I have examined the effect of denaturants and reducing agents on the fluorescence signals. I have begun studying the effect of heparin on the fluorescence signal. There is no large change in the  $\lambda_{\text{max}}$  emission, but there is a slight change in intensity of the signal. The effect on the trp micro-environment appears to be small. The effect of external quenchers to the trp micro-environment still needs to be addressed. I have also begun to study the effect of DTT on the CD signal of P3 and P123. Under the guidance of Dr. Ivan Rayment, I plan to begin technical objective 5- a crystallization trial of the type 1 repeats. However, I will need to isolate more protein prior to initiating this study. The biophysical techniques require a large amount of purified protein and the crystallography will require even more. Hanging-drop vapor diffusion using 102 different solutions at room temperature and 4°C will be the method for crystal growth.

## VII. Conclusions

### A. Expression of P3 and P123:

1. The expression of P123 was >20mg/L while that of P3 was 1-2mg/L.
2. The use of the pCOCO expression system allowed P3 and P123 to be purified from conditioned media (CM) of baculovirally infected High 5 cells in the absence of denaturants. P123 could be directly purified from the CM while the low expression of P3 required the CM to be concentrated.
3. The proteins were pure as determined by SDS-PAGE and MALDI-TOF MS.

### B. The N-Terminus of both P3 and P123 are homogeneous and the GP67 signal sequence was cleaved at the anticipated site.

**C. Mass determination by MALDI-TOF MS:**

1. At least, four masses were determined for P3 and at least two masses were associated with P123. The first peak mass for P3 and P123 are slightly below the expected mass based on the knowledge of the N-terminus, the cDNA, and the thrombin cleavage site at the C-terminus. It is possible that the loss of ~18Da per type 1 repeat is due to modification of conserved serine, aspartic acid, or asparagine residues.
2. The multiple masses determined for either P3 or P123 could be due to the presence of O-linked glycosylation. The difference in mass between the peaks is 156-164 Da, which is within the mass range for a single sugar. In addition, the use of the DIG Glycan Detection system has shown both P3 and P123 to be glycosylated.

**D. Disulfide Bond Content of P3 determined by MALDI-TOF MS:**

1. No free thiols are present in P3 since there was no mass shift of the native or denatured P3 following labeling with iodoacetic acid.
2. P3 has 6 cys and they are in disulfide bonds. Only P3 that was treated with reducing agent, in the presence or absence of GuHCl, and then labeled with iodoacetic acid had an increase in mass of six times the mass of iodoacetic acid.

**E. The Far-UV CD Spectra of P3 and P123:**

1. The spectra for P3 and P123 are marked by distinctive positive ellipticity that could in part be due to trp contribution. The two positive signals are also seen in the complement protein properdin which contains six type 1 repeats in series .
2. Heating P3 or P123 causes a transition to a random coil conformation.
3. The Far-UV CD spectra of P3 and P123 at 25°C plotted as molar ellipticity (mean residue weight) are very similar.

**F. The Near-UV CD Spectra of P3 and P123:**

1. The spectra for P3 and P123 are marked by positive ellipticity. The peak centered about 280nm is due to the trps, since neither P3 and P123 have tyrosine.
2. Heating P3 or P123 to 55°C eliminates the chirality of the trps.
3. The Near-UV CD spectra of P3 and P123 at 25°C plotted as molar ellipticity (mean residue weight) are very similar in shape. However, P123 is approximately two-thirds the intensity of P3. There is an overall difference in the chirality of the 9 trps in P123 compared to the three trps in P3.

**G. Dual monitoring of CD and Fluorescence of P123:**

1. Heating P123 for 25°C->75°C causes a decrease in the CD signal at 210nm and an increase in the total fluorescence emission.
2. The unfolding of P123 appears to be cooperative.
3. These results are similar to those observed using P3.

**H. Fluorescence Emission Spectra of P3 and P123:**

1. The wavelength of maximum emission ( $\lambda_{\max}$ ) for P3 and P123 are very similar, 332-333nm. The environment of the trps in P3 and P123 would be expected to be slightly non-polar.
2. Upon reduction of the disulfides with DTT or denaturation of P3 or P123 with 6M GuHCl, there is a large enhancement in total fluorescence and a large red-shift in  $\lambda_{\max}$ .  
In the native conformation, the disulfides appear to quench and the trps are in a less polar environment compared to the denatured or reduced state.
3. The transition induced by DTT on the conserved Trp is rapid and complete within ~20minutes. However, the effect of DTT on the secondary structure appears to be slower, taking hours at 25°C to reach completion.

## VIII. References

1. P. Bornstein, K. O'Rourke, K. Wikstrom, F. W. Wolf, R. Katz, et al, *J. Biol. Chem.* **266**, 12821 (1991).
2. C. M. Verfaillie, W. J. Miller, K. Boylan, P. B. McGlave, *Blood* **79**, 1003 (1992).
3. J. Lawler, M. Duquette, C. A. Whittaker, J. C. Adams, K. McHenry, et al, *J. Cell Biol.* **120**, 1059 (1993).
4. A. Oldberg, P. Antonsson, K. Lindblom, D. Heinegard, *J. Biol. Chem.* **267**, 22346 (1992).
5. A. Klar, M. Baldassare, T. M. Jessell, *Cell* **69**, 95 (1992).
6. J. Lawler, L. H. Derick, J. E. Connolly, J-H. Chen, F. C. Chao, *J. Biol. Chem.* **260**, 3762 (1985).
7. J. Lawler, R. O. Hynes, *J. Cell Biol.* **103**, 1635 (1986).
8. J. Lawler, E. R. Simons, *J. Biol. Chem.* **258**, 12098 (1983).
9. M. J. Bissell, H. G. Hall, G. Parry, *J. Theor. Biol.* **99**, 31 (1982).
10. P. L. Jones, C. Schmidhauser, M. J. Bissell, *Crit. Rev. Eukaryot. Gene Expr.* **3**, 137 (1993).
11. R. J. Blaschke, A. R. Howlett, P. Y. Desprez, O. W. Petersen, M. J. Bissell, *Methods Enzymol.* **245**, 535 (1994).
12. C. D. Roskelley, P. Y. Desprez, M. J. Bissell, *Proc. Natl. Acad. Sci. U. S. A.* **91**, 12378 (1994).
13. C. Pechoux, P. Clezardin, R. Dante, C. M. Serre, M. Clerget, et al, *Differentiation* **57**, 133 (1994).
14. P. Clezardin, L. Frappart, M. Clerget, C. Pechoux, P. D. Delmas, *Cancer Res.* **53**, 1421 (1993).
15. J. Dawes, P. Clezardin, D. A. Pratt, *Sem. Thromb. Hemost.* **13**, 378 (1987).
16. V. Zabrenetzky, C. C. Harris, P. S. Steeg, D. D. Roberts, *Int. J. Cancer* **59**, 191 (1994).
17. D. L. Weinstat-Saslow, V. S. Zabrenetzky, K. VanHoutte, W. A. Frazier, RobertsDD., et al, *Cancer Res.* **54**, 6504 (1994).
18. S. S. Tolsma, O. V. Volpert, D. J. Good, W. A. Frazier, P. J. Polverini, et al, *J. Cell Biol.* **122**, 497 (1993).
19. D. J. Good, P. J. Polverini, F. Rastinejad, M. M. Le Beau, R. S. Lemons, et al, *Proc. Natl. Acad. Sci. U. S. A.* **87**, 6624 (1990).
20. P. Bagavandoss, J. W. Wilks, *Biochem. Biophys. Res. Comm.* **170**, 867 (1990).
21. T. Vogel, N-H. Guo, H. C. Krutzsch, D. A. Blake, J. Hartman, et al, *J. Cell. Biochem.* **53**, 74 (1993).
22. F. W. Wolf, R. L. Eddy, T. B. Shows, V. M. Dixit, *Genomics* **6**, 685 (1990).
23. C. A. Smith, M. K. Pangburn, C. W. Vogel, H. J. Muller-Eberhard, *J. Biol. Chem.* **259**, 4582 (1984).
24. R. W. Woody, *Biopolymers* **17**, 1451 (1978).
25. R. W. Woody, *Eur. Biophys. J.* **23**, 253 (1994).

**Figure 1: Trimeric Organization of TSP1**

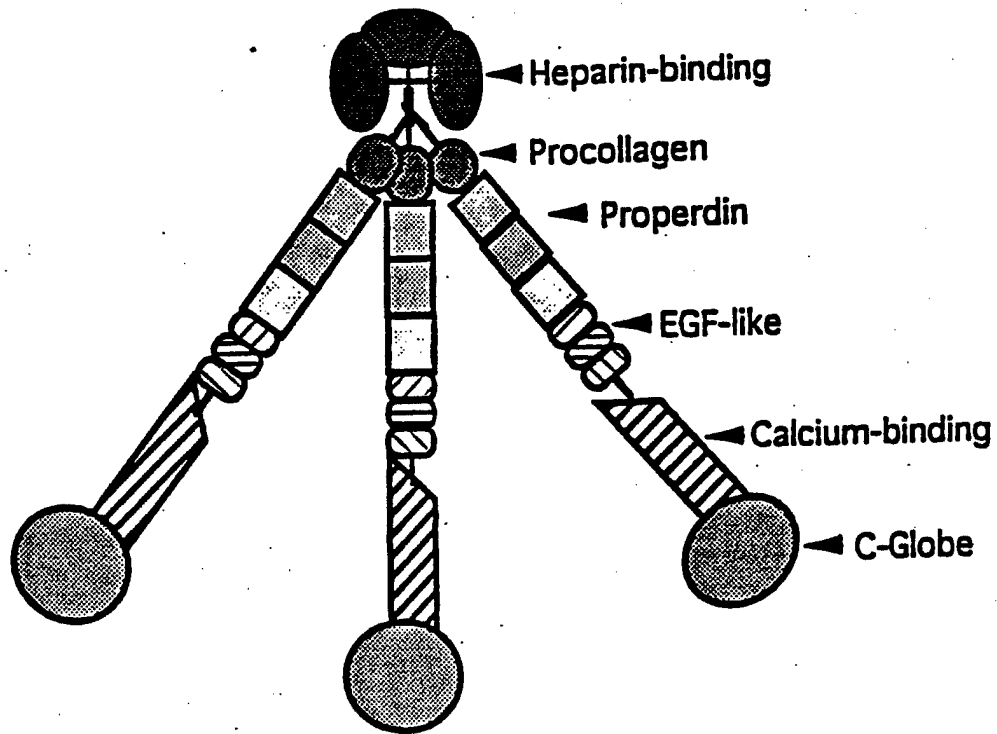


**Figure 2: Amino Acid Sequence of hTSP1 Type 1 Repeats**

		1	2	3	4	5	6
1st	SDSADDG	<b>WSPWSE</b>	WTSCST	SCGNGIQ	QRGRSCD	SLNNR	....CEGSSVQTRTCHIQC
2nd	KQDGG	<b>WSPWSS</b>	CSVTCG	DGVI	TRIRLCNS	PSPQMNGK	PCEGEARETKACKKDACP
3rd	NGG	<b>WSPWDI</b>	CSVTCG	GGVQKR	SRLC	<u>NP</u> TPQFGGKDC	VGDVTENQICNKQDCPID

**Figure 3: Features of Baculovirus Transfer Vector pCOCO**

	<b>Thrombin Site</b>	<b>Histidine-Tag</b>
<b>Protein</b>	L E <u>L V P R G S</u> A A G	<u>H H H H H H H</u> Z
<b>DNA</b>	t c t a g a a t t a g t g c c t c g c g g a a g c g c t g c a g g g	c a t c a c c a t c a c c a t c a c t a g g a c c t a c t
	<b>XbaI</b>	<b>PstI</b>
		<b>PpumiI</b>

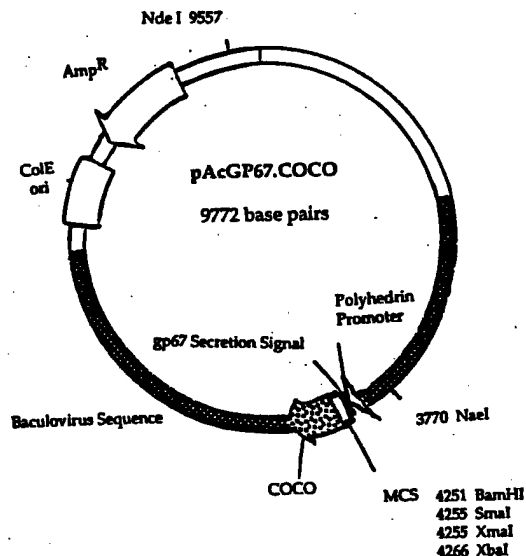


**Figure 4: Fusion Proteins Expressed using pCOCO**

			<b>Thrombin Site</b>	<b>His-Tag</b>	<b>Size (kDa)</b>
<b>General</b>	ADPG	(-----INSERT-----)	L E L V P R G S A A G	<u>H H H H H H H H H</u>	
<b>P123.COCO</b>	ADPG		L E L V P R G S A A G	<u>H H H H H H H H H</u>	21.1
<b>P3.COCO</b>		ADPG	L E L V P R G S A A G	<u>H H H H H H H H H</u>	8.4
<b>Post-Thrombin Cleavage</b>					
<b>P123.C</b>	ADPG		L E L V P R		20.0
<b>P3.C</b>		ADPG	L E L V P R		7.3

## Figure 5: N-Terminal Sequence Determination

### A. Amino Acid Sequences of Constructs

#### 1. P123.COCO

|-----Proposed GP67 signal sequence-----|

```

1   MLLVNQSHQGFNKEHTSKMVSATVLYVLLAAAAHSAFAADPGSDSADDGW
51  SPWSEWTSCSTSCNGIQQRGRSCDSLNNRCEGSSVQTRTCHIQECDKRF
101 KQDGGWSHWSPWSSCSVTCGDGVI TRIRLCNSPSPQMNGKPCEGEARETK
151 ACKKDACPINGGWGPWSPWDICSVTCGGGVQKRSRLCENNPTPQFGGKDCV
201 GDVTENQICNKQDCPILELVPRGSAAGHHHHHH

```

#### 2. P3.COCO

|-----Proposed GP67 signal sequence-----|

```

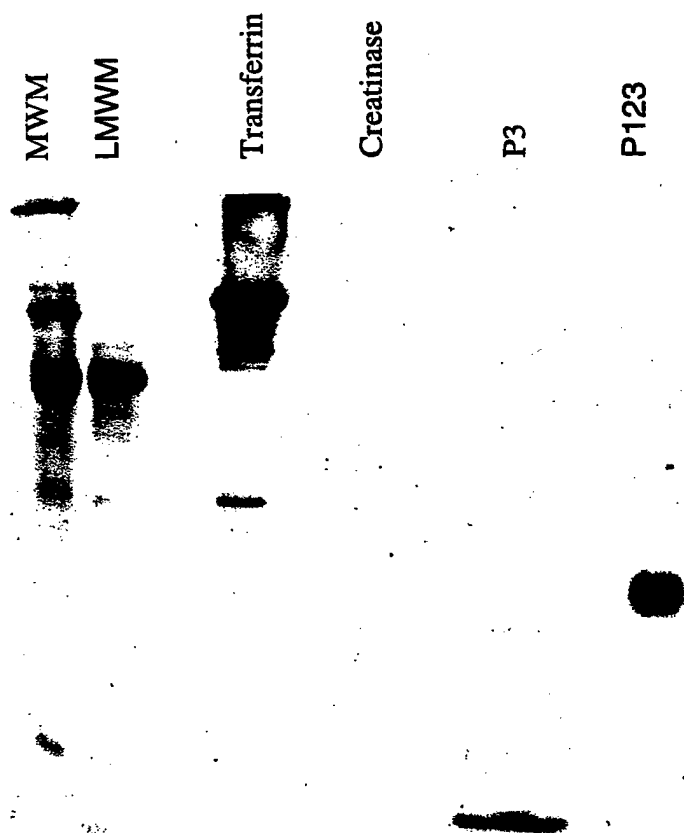
1   MLLVNQSHQGFNKEHTSKMVSATVLYVLLAAAAHSAFAADPGINGGWGPW
51  SPWDICSVTCGGGVQKRSRLCENNPTPQFGGKDCVGDVTENQICNKQDCPI
101 LELVPRGSAAGHHHHHH

```

### B. Results of N-Terminal Sequence Analysis

Cycle	Sequenced from P123	Match	Sequenced from P3	Match
1	A	+++	A	+++
2	D	+++	D	+++
3	P	+++	P	+++
4	G	+++	G	+++
5	S	+++	I	+++
6	D	+++	N	+++
7	S	+++	G	+++
8	A	+++	G	+++
9	D	+++		
10	D	+++	P	+++

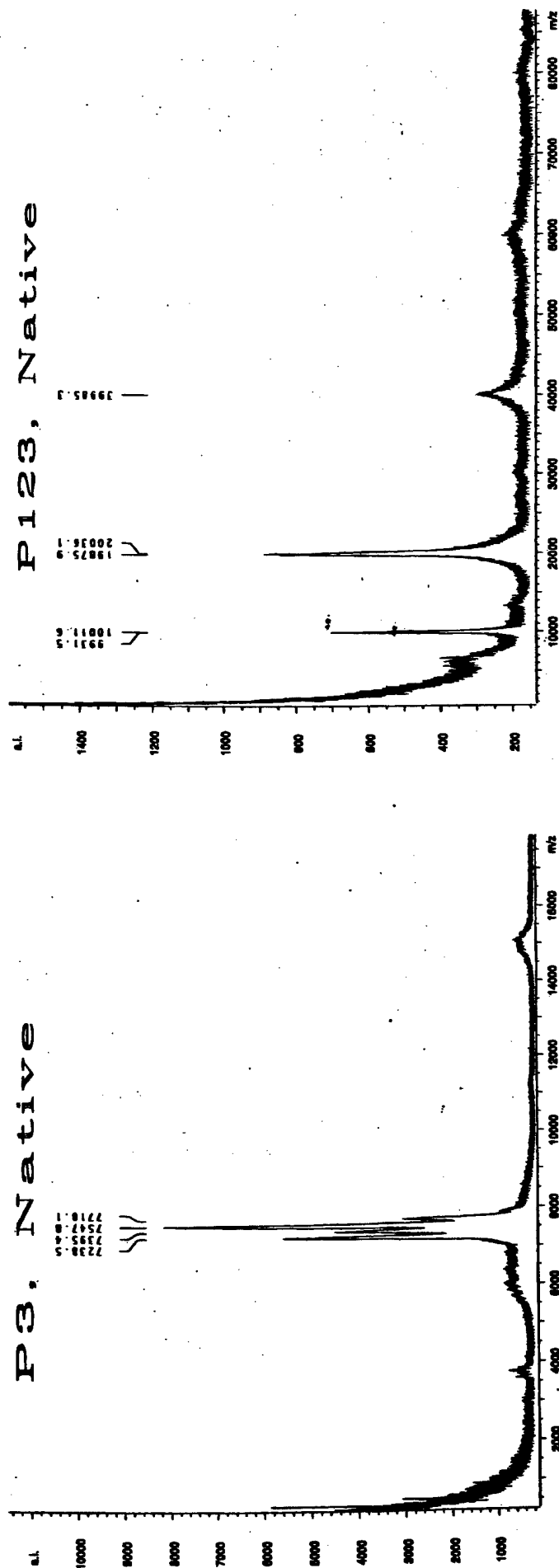
**Figure 6: DIG Glycan Western Blot of P3 and P123**



Immunoblot of P3 and P123 using anti-DIG-alkaline phosphatase conjugated antibody. Samples were denatured with SDS, reduced with BME, and boiled for 10 minutes prior to loading on a 14% SDS-PAGE. The proteins were transferred to nitrocellulose and DIG modification and detection were performed according to the manufacturer's instructions. MWM, Molecular Weight Markers; LMWM, Low Molecular Weight Markers; Transferrin, Positive Control glycoprotein; Creatinase, Negative control non-glycosylated protein; P3, Purified; P123, Purified.

**Figure 7: Mass Determination of P3 and P123 by MALDI-TOF Mass Spectroscopy**

Protein	Average Mass Peak 1	Average Mass Peak 2	Average Mass Peak 3	Average Mass Peak 4
P3	7254.3 Da	7410.4 Da	7562.0 Da	7726.4 Da
P123	19919.0 Da	20077.7 Da		



Molecular Mass Determination of P3 and P123 by MALDI-TOF. The data were collected on a Bruker matrix-assisted laser desorption ionization, time-of-flight mass spectrometer. The proteins were dialyzed extensively into 5% acetic acid and then lyophilized. The proteins were resuspended in water to a concentration of 10-40 pmol/ul. The matrix was  $\alpha$ -cyano-4-hydroxycinnamic acid at 10mg/ml. Internal calibrants of insulin, ubiquitin, and/or trypsinogen were used to determine the masses. The table lists the average mass determined from several independent experiments. Representative spectra for P3 and P123 without calibrants are also shown.

**Figure 8: P3 is Disulfide Bonded and Contains No Free Thiols**

Treatment	Mass of 1st Peak	$\Delta$ Mass wrt Native	$\Delta$ Mass/ Mass IA	Number of Cys Labeled
Native	7246.5 Da	0.0 Da	0.0	0.0
DTT/IA	7597.1 Da	350.6 Da	6.04	6.04
GuHCl/IA	7251.9 Da	5.4 Da	0.09	0.09
DTT/GuHCl/IA	7599.2 Da	352.7 Da	6.08	6.08

Determination of the Disulfide Bond Content of P3 MALDI-TOF. The data were collected on a Bruker matrix-assisted laser desorption ionization, time-of-flight mass spectrometer. The P3 protein was labeled for 30 minutes with Iodoacetic acid (IA) under four conditions: Native; 6mM DTT; 6M Guanidine Hydrochloride; and 6M Guanidine Hydrochloride and 6mM DTT. The protein was equilibrated in each of the four conditions for 90 minutes under nitrogen gas prior to labeling with IA. Following labeling the proteins were dialyzed into 5% acetic acid and then lyophilized. The proteins were resuspended in water to a concentration of 10-20 pmol/ul. The matrix was  $\alpha$ -cyano-4-hydroxycinnamic acid at 10mg/ml. Internal calibrants of insulin and ubiquitin were used to determine the masses. The table lists the mass determined for the first peak of P3 for each treatment condition. The calculated mass difference relative to the first peak of native P3 and the resulting number of Cys labeled by IA are also listed.

**Figure 9: Far-UV CD Circular Dichroism of P3 and P123**

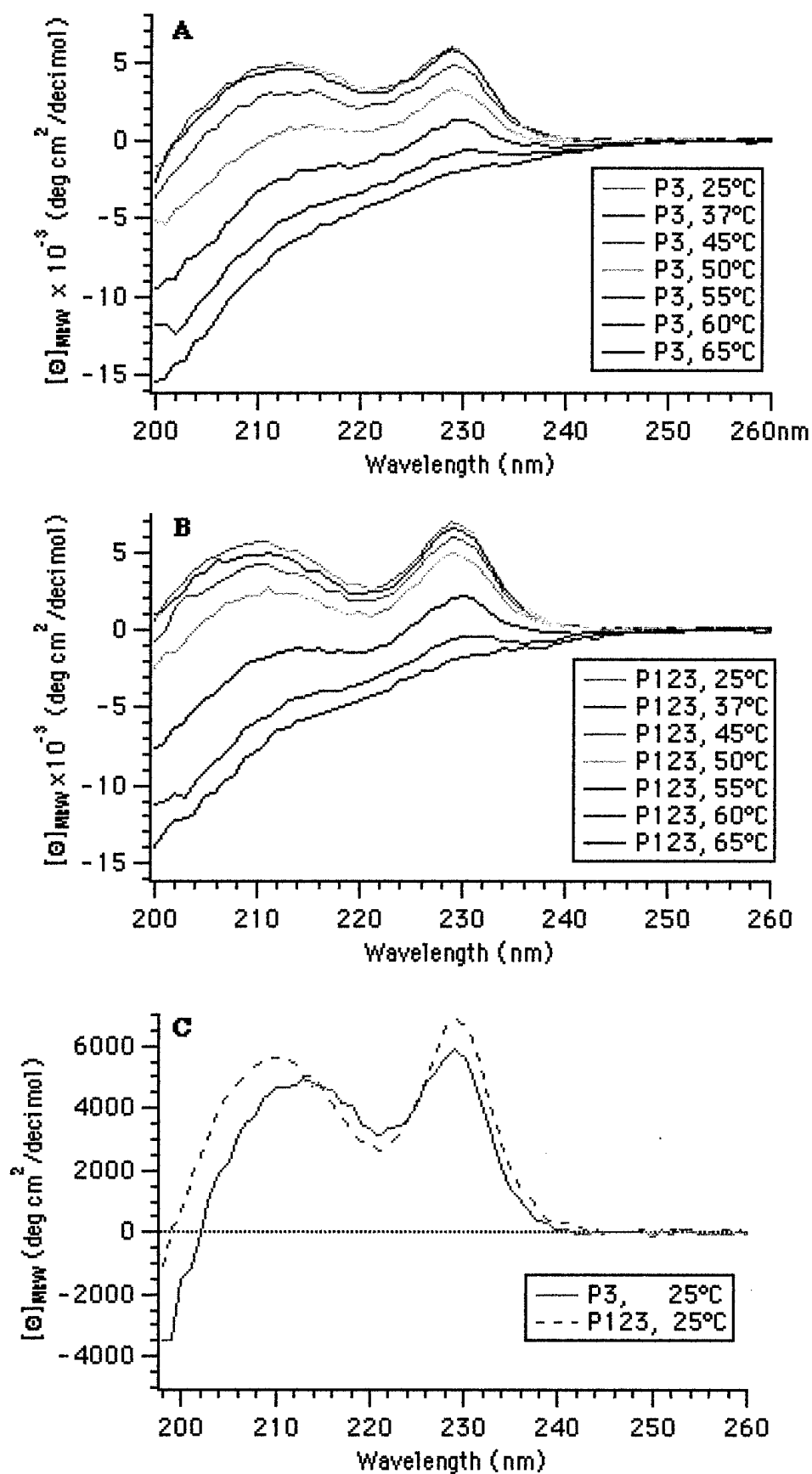


**Figure 10: Near-UV Circular Dichroism of P3 and P123**

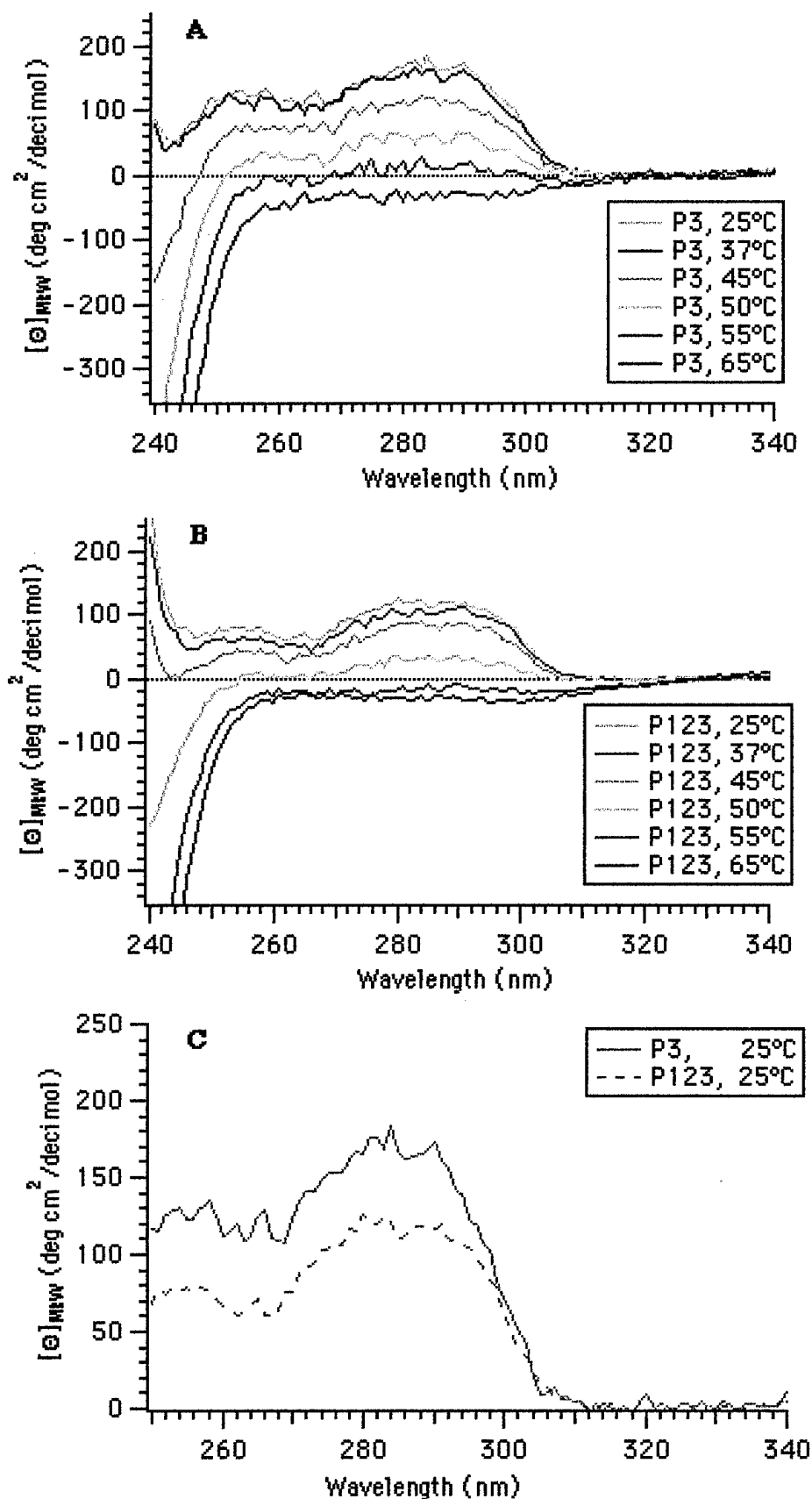


**Figure 11: Dual Monitoring of CD and Fluorescence Signals of P123 with Increasing Temperature**

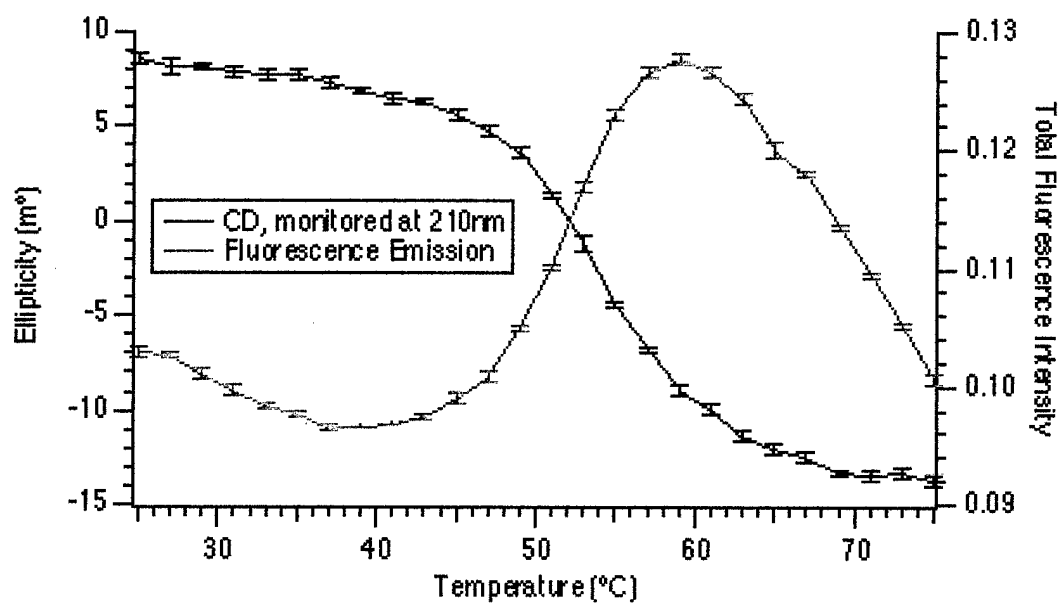


**Figure 12: Fluorescence Emission Spectra of P3 and P123 under Native and Denaturing Conditions**

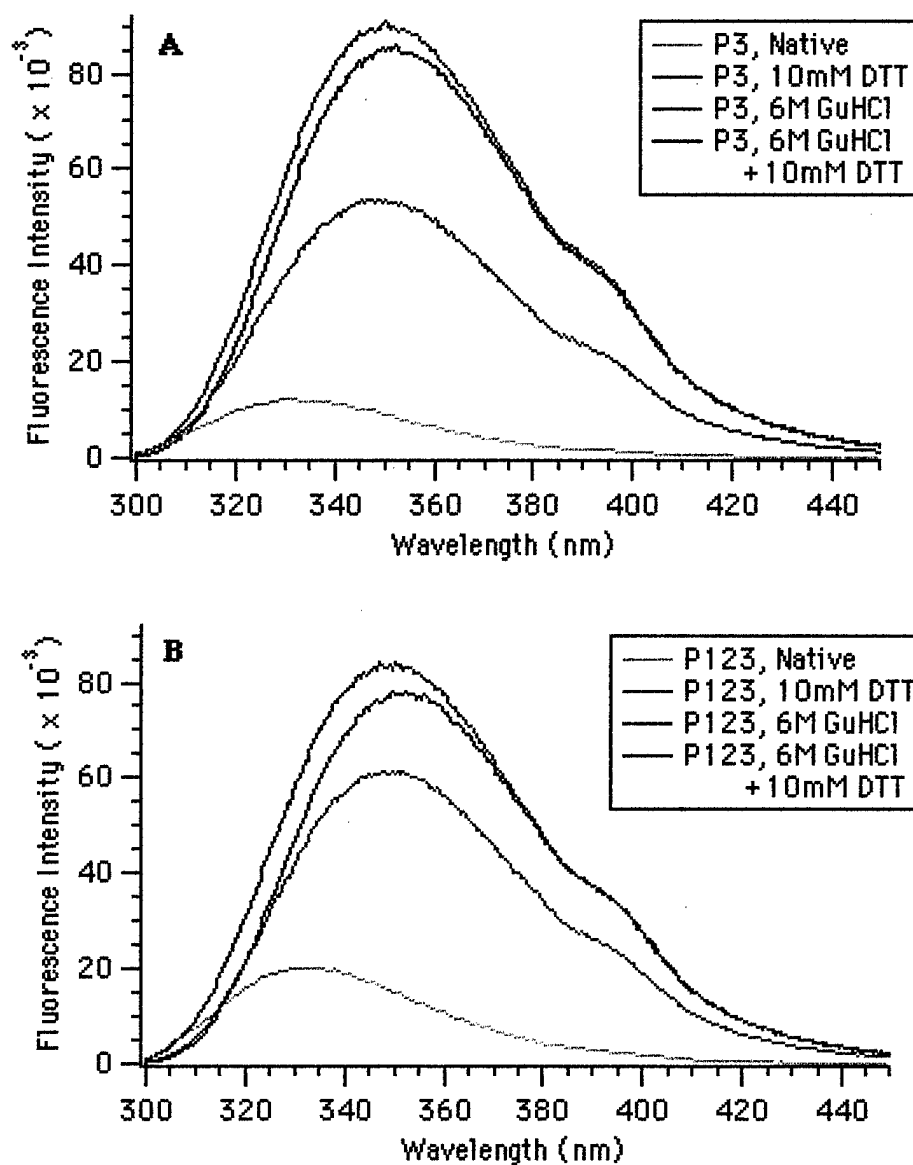


**Figure 12: Fluorescence emission Spectra of P3 and P123 under Native and Denaturing Conditions**

**C. Summary of the Wavelength of Maximum Emission for P3 and P123**

Protein	Emission $\lambda_{max}$			
	Native	+ 10 mM DTT	+ 6 M GuHCl	+ 6 M GUHCl + 10 mM DTT
P3	332 nm	349 nm	350 nm	352 nm
P123	333 nm	349 nm	347 nm	352 nm

**D. Shift in the Wavelength of Maximum Emission Induced by Titration with DTT**

